THE JOURNAL OF PHYSICAL CHEMISTRY A
A JOURNAL OF THE AMERICAN CHEMICAL SOCIETY

pubs.acs.org/JPCA Article

Semiclassical Vibrational Spectroscopy of Real Molecular Systems by Means of Cross-Correlation Filter Diagonalization

Jia-Xi Zeng, Shuo Yang, Yu-Cheng Zhu,* Wei Fang, Ling Jiang, En-Ge Wang, Dong H. Zhang, and Xin-Zheng Li*

Cite This: J. Phys. Chem. A 2023, 127, 2902−2911 Read Online

ABSTRACT: We applied the harmonic inversion technique to extract vibrational eigenvalues from the semiclassical initial value representation (SC-IVR) propagator of molecular systems described by explicit potential surfaces. The cross-correlation filter-diagonalization (CCFD) method is used for the inversion problem instead of the Fourier transformation, which allows much shorter propagation time and is thus capable of avoiding numerical divergence issues while getting rid of approximations like the separable one to the pre-exponential factor. We also used the "Divide-and-Conquer" technique to control the total dimensions under consideration, which helps to further enhance the numerical behavior of SC-IVR calculations and the stability of harmonic inversion methods. The technique is tested on small molecules and water trimer to justify its applicability and reliability. Results show that the CCFD method can effectively extract the vibrational eigenvalues from short trajectories and reproduce the original spectra conventionally obtained from long-time ones, with no loss on accuracy while the numerical behavior is much better. This work demonstrates the possibility to apply the combined method of CCFD and SC-IVR to real molecular potential surfaces, which might be a new way to overcome the numerical instabilities caused by the increase of dimensions.

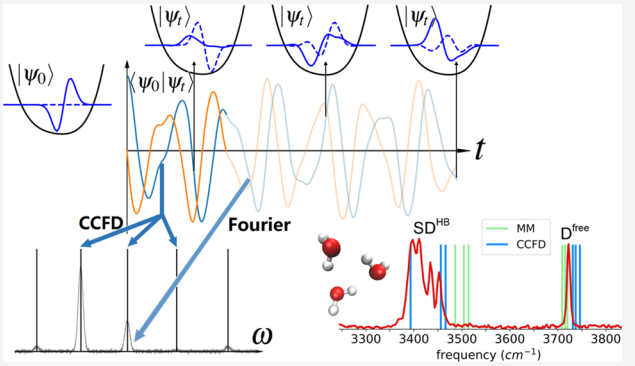

INTRODUCTION

In theoretical studies of the dynamical properties of the nuclei in polyatomic systems, especially vibrational spectra, molecular dynamics (MD) is a method of standard choice.[1−3] In this method, the nuclei are treated as mass points moving on a potential energy surface (PES) where the electronic degrees of freedom are solved independently to yield the potential energy and the atomic forces.[4,5] The nuclear trajectories are generated with specified ensembles and evolved under classical equations of motion, and statistical quantities are extracted from them, including the configurational and dynamical ones. In recent years, it was noticed that the complete neglect of the quantum nature of the nuclei keeps bare MD simulations from recovering many interesting nuclear quantum effects (NQEs) including those related to anharmonic corrections, to zero-point motion,[6] and to interference and tunneling.[7] The effects are important in several systems, especially when hydrogen is involved.[8,9] Therefore, new method which goes beyond the classical treatment of the nuclei is highly desirable in accurate theoretical simulations.

So far, many methods have been developed which handle atoms by means of wave functions or path integrals. Among them are multiconfiguration time-dependent Hartree (MCTDH),[10−13] vibrational self-consistent field (VSCF)[14−17] and vibrational configuration interaction (VCI).[16,17] In these methods, the nuclear wave functions are expressed as combinations of the direct products of "single-particle" functions. The Schrödinger equation is solved under this basis, so that the energy levels of the nuclear states or the evolved nuclear wave functions are obtained. The computational effort of these methods grows exponentially with the total degrees of freedom, which posted a strong limit on their application to complex systems.[18] Another category of methods includes those involving statistics. The Diffusion Monte Carlo (DMC) method approaches the nuclear wave functions by the spawn and annihilation of diffusing particles.[19−21] The path-integral based methods, e.g., Centroid Molecular Dynamics (CMD) and Ring-Polymer Molecular Dynamics (RPMD), make accurate quantum statistics by

Received: January 26, 2023
Revised: March 6, 2023
Published: March 23, 2023

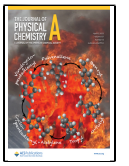

https://doi.org/10.1021/acs.jpca.3c00576
J. Phys. Chem. A 2023, 127, 2902−2911

inserting harmonically connected beads and record snapshots of the moving polymer as samples.[22−24] These methods have their strengths but also limitations. DMC is very accurate about the ground state but encounters difficulties for excited states with nodes. RPMD suffers from spurious resonances from the harmonic chain frequencies. CMD has its own curvature problem which originates from the nonphysical centroid position. Their computational cost all grow heavy at low temperatures where a large number of beads are required.[23,24]

Parallel to them, the semiclassical initial value representation (SC-IVR) also shows promise in dealing with molecular vibrational spectra with NQEs accurately addressed.[25,26] The origin of this method can be traced back to the first half of the last century.[27] In the last few decades, great progresses have been achieved.[26] Starting from the semiclassical approximation to the quantum propagator,[27] the evolution of the nuclear wave function can be reformulated in terms of the classical dynamics on the same potential surface. The transformation from the root-searching form to the initial value representation has finally made the method realistically available for numerical computation.[25,26] Being capable of handling interference and anharmonic effect, it is a promising tool based on conventional molecular dynamics.

However, in practice, it also suffers from many problems such as the curse of dimensionality. The computational work required to get a spectra grows still fast with dimension. The "Divide-and-Conquer" technique is a successful example which was proposed in recent years to simulate the relatively large systems.[28−30] This method projects the whole phase space to a low-dimensional subspace while still keeping part of information from the original full-dimensional system. By properly choosing the subspace division criterion,[29] it is possible to keep most of the useful information while immensely reducing the dimension under consideration. Lowering the total dimension significantly saves computational resources and also benefits numerical stability and convergence. With this technique one can even deal with sizable biological systems.[31]

Besides coping directly with the dimensionality, various other modifications have also been made to reduce the computational cost. The TA-SC-IVR method is one example, which features a time-averaging filter that efficiently reuses the trajectory data and meanwhile ensures a positive definite integrand.[32,33] It is numerically friendly for a Monte Carlo sampling. The MC-SC-IVR method uses superposition of multiple coherent states as the reference state, which enhances the overlapping signal and allows for some symmetry selection.[34] Both methods significantly reduce the number of trajectories required to achieve numerical convergence. Other techniques for reducing the overall computational work include the Adiabatic Switching technique which helps to preprocess the dynamics and improve the initial sample distribution,[35,36] as well as the Hessian database method[37] and the finite displacement evaluation of monodromy matrix.[38]

Concerning the extraction of the spectrum from the molecular dynamics trajectories, harmonic inversion which restores the parameters of oscillators from time-domain signals is an often used method. Along this route, current methods in SC-IVR generally use Fourier transform, which requires evolving the trajectories for a typical total length of $\sim 10^5$ atomic units.[28,33,34] At this time scale, the use of approximations on the pre-exponential factor such as the separable approximation is forced; otherwise, its value will grow too large and make numerical convergence infeasible.[39] The propagation of the monodromy matrix also encounters numerical stiffness, so that one has to discard a considerable portion of the trajectories.[29] If one can reduce the total evolving time to $\sim 10^3$ atomic units, the absolute value of the pre-exponential factor and the monodromy matrix element will be kept within a reasonable range, and the numerical convergence will be much easier to achieve in the simulations.

To recover the vibrational spectrum from short-time signals, Fourier transform is no longer appropriate due to its poor resolution. Several alternative numerical methods have been developed.[40] One important thing to notice and exploit here is that the energy spectra of a bounded system is discrete, so that, for an ideal molecular vibrational spectra, the intensity shall be composed of impulse function peaks located at the energy eigenvalues. For a particular reference state, the number of main peaks with non-negligible strength is limited to a few, making the time-domain signal almost a combination of simple oscillators. In other words, the resulting energy spectrum is relatively sparse on the frequency domain. Even if there are various source of error in the computational process which makes the resulting spectrum no longer an ideal one, in most cases we can still be confident that there are only sharp and almost separated peaks. Thus, by information theory, it is possible to extract those peaks from very short trajectories due to the significant reduction for needed information.

The filter-diagonalization method (FDM) is designed to extract eigenvalues from the matrix elements of propagators on a small basis.[41] It uses an implicit basis set which is derived from reference states by the action of a finite-time propagator. The eigenvalues are extracted by diagonalizing the propagator in the vector space spanned by this implicit basis. Using this method, the vibrational frequencies can be obtained from cross-correlation functions of several reference states on a small time grid.[42−44] Therefore, it can work as a postprocessing tool for analyzing the data generated by SC-IVR method. It is worth noting that it is even possible to identify very closely spaced peaks and also supports classification by symmetry with some preconditioning techniques.[43,44] The combination of the SC-IVR and FDMs has been previously tested on some model Hamiltonians[45−47] but not yet applied to realistic molecular potential energy surfaces. However, there seems to be no reason that it cannot work on larger systems and more sophisticated PESs. With the modern high-accuracy force models, one can expect to get spectra of good precision with the method.

This paper is organized as follows. In Theory and Methods, we introduce the basic ideas and methods we used in the overall procedure of calculation. In Results and Discussion, we present the results we obtain. These results include the vibrational spectrum derived from simple models as well as several real PESs, the convergence test, and error analysis of the method. The comparison with experimental data and other similar methods will also be discussed. In the Conclusion, a brief summary of the conclusions is given.

THEORY AND METHODS

Semiclassical Initial Value Representation. The quantum propagator under semiclassical approximation and initial value representation takes the form of a phase-space integral[48]

https://doi.org/10.1021/acs.jpca.3c00576
J. Phys. Chem. A 2023, 127, 2902−2911

$$e^{-i\hat{H}t} = \int d\mathbf{q}_0 \int d\mathbf{p}_0 \left[\left| \frac{\partial \mathbf{q}_t}{\partial \mathbf{p}_0} \right| / (2\pi i\hbar)^D \right]^{1/2} \times e^{iS_t(\mathbf{q}_t,\mathbf{q}_0)/\hbar} |\mathbf{q}_t\rangle\langle \mathbf{q}_0| \quad (1)$$

where D means the degree of freedom. This equation can be carried out by omitting higher order terms of $\hbar$ in the Schrodinger equation[27] and transforming variables to the initial phase space[26] and also can be derived from stationary phase approximation of the real-time path integral.[49] This semiclassical propagator is exact in the case of free particle and harmonic oscillator and has good accuracy in many general situations.

A useful variation of the expression is the coherent state representation developed by Herman and Kluk[26,48]

$$e^{-i\hat{H}t/\hbar} = \frac{1}{(2\pi\hbar)^F} \int d\mathbf{p}_0 \int d\mathbf{q}_0 \, C_t(\mathbf{p}_0, \mathbf{q}_0) \times e^{iS_t(\mathbf{p}_0,\mathbf{q}_0)/\hbar} |\mathbf{p}_t, \mathbf{q}_t\rangle\langle \mathbf{p}_0, \mathbf{q}_0| \quad (2)$$

Here $\mathbf{q}_t$, $\mathbf{p}_t$ is the coordinate and momentum at time t, S_t is the action along the path

$$S_t(\mathbf{p}_0, \mathbf{q}_0) = \int_0^t dt' \, \mathbf{p}_{t'}\dot{\mathbf{q}}_{t'} - H(\mathbf{p}_{t'}, \mathbf{q}_{t'}) \quad (3)$$

and C_t is the Herman−Kluk pre-exponential factor

$$C_t(\mathbf{p}_0, \mathbf{q}_0) = \sqrt{\frac{1}{2^D} \left| \frac{\partial \mathbf{q}_t}{\partial \mathbf{q}_0} + \Gamma^{-1}\frac{\partial \mathbf{p}_t}{\partial \mathbf{p}_0}\Gamma - i\hbar\frac{\partial \mathbf{q}_t}{\partial \mathbf{p}_0}\Gamma + \frac{i}{\hbar}\Gamma^{-1}\frac{\partial \mathbf{p}_t}{\partial \mathbf{q}_0} \right|} \quad (4)$$

All time-dependent quantities are evaluated by classical dynamics, with initial conditions $\mathbf{q}_0$, $\mathbf{p}_0$. That is, the integrand in eq 2 is a function of the initial position and momentum of the nuclei and can be derived from the classically evolved trajectory.

The coherent states are minimum-uncertainty wave packets with wave function

$$\langle \mathbf{x}|\mathbf{p}, \mathbf{q}\rangle = \left(\frac{\det \Gamma}{\pi^D}\right)^{1/4} e^{-(1/2)(\mathbf{x}-\mathbf{q})^T\Gamma(\mathbf{x}-\mathbf{q})+i/\hbar\mathbf{p}^T(\mathbf{x}-\mathbf{q})} \quad (5)$$

Γ is the width matrix of the coherent state, which is usually chosen to coincide with the case of quantum harmonic oscillators. The ground state under harmonic approximation can then be written as $|\mathbf{0}, \mathbf{q}_{eq}\rangle$, where $\mathbf{q}_{eq}$ is the equilibrium position of lowest energy. For a reference state $|\chi\rangle$, its surviving amplitude is defined as

$$A_\chi(t) \equiv \langle \chi|e^{-i\hat{H}t/\hbar}|\chi\rangle \quad (6)$$

The energy spectrum of this $|\chi\rangle$ can be achieved by its Fourier transformation, through

$$\begin{aligned} I(E) &\equiv \langle \chi|\delta(E-\hat{H})|\chi\rangle \\ &= \frac{1}{\pi\hbar}\,\mathrm{Re}\int_0^\infty dt\, e^{iEt/\hbar}\langle \chi|e^{-i\hat{H}t/\hbar}|\chi\rangle \\ &= \frac{1}{\pi\hbar}\,\mathrm{Re}\int_0^\infty dt\, e^{iEt/\hbar}A_\chi(t) \end{aligned} \quad (7)$$

Combining eqs 2, 6, and 7, we obtain the expression of the semiclassical energy spectra

$$I_\chi(E) = \frac{1}{(2\pi\hbar)^D}\frac{1}{\pi\hbar}\,\mathrm{Re}\int_0^\infty dt\, e^{iEt/\hbar}\int d\mathbf{p}_0 \int d\mathbf{q}_0\, C_t(\mathbf{p}_0, \mathbf{q}_0) \times e^{iS_t(\mathbf{p}_0,\mathbf{q}_0)/\hbar}\langle \chi|\mathbf{p}_t, \mathbf{q}_t\rangle\langle \mathbf{p}_0, \mathbf{q}_0|\chi\rangle \quad (8)$$

This expression is sufficient for a Monte Carlo integration in the phase space for simple systems. The inner product factor is a valid candidate of the weighing function. Here, the reference state is usually chosen to be linear combinations of the coherent states in order to have an analytical Gaussian form for the overlapping term. For long trajectories, it is often the case that the pre-exponential factor be evaluated using some kind of approximation to ensure numerical stability. But, in this paper, we will just use the exact form.

Divide-and-Conquer SC-IVR. The Divide-and-Conquer method is a technique to circumvent the curse of dimensionality, in which the original system is projected onto a small subset of its dimensions and many parts of the expressions are written in subspace coordinates.[28,29] The formula of energy spectrum is very similar to the original one,

$$e^{-i\hat{H}t/\hbar} = \frac{1}{(2\pi\hbar)^D} \int d\tilde{\mathbf{p}}_0 \int d\tilde{\mathbf{q}}_0 \, \tilde{C}_t(\tilde{\mathbf{p}}_0, \tilde{\mathbf{q}}_0) \times e^{i\tilde{S}_t(\tilde{\mathbf{p}}_0,\tilde{\mathbf{q}}_0)/\hbar} |\tilde{\mathbf{p}}_t, \tilde{\mathbf{q}}_t\rangle\langle \tilde{\mathbf{p}}_0, \tilde{\mathbf{q}}_0| \quad (9)$$

except for the tilde variables which are projections of the corresponding quantities in eq 2. The other formulas eqs 3−5 shall also be reformulated based on projection.[29] Despite the straightforward basis contraction of the vectors and matrices, the potential term in the Hamiltonian is not separable and thus cannot be directly projected and requires special treatment. A common ad hoc method is to assume

$$\tilde{V}(\tilde{\mathbf{q}}) = V(\mathbf{q}) - V(\tilde{\mathbf{q}}; \mathbf{q}_{D-\tilde{D}}) \quad (10)$$

where $\mathbf{q}_{D-\tilde{D}}$ is the complement of the projected coordinates, so that the projected potential is exact for separable cases.[28,29] $\tilde{V}$ is not a single-valued function. It accounts for the coupling effects of the ignored dimensions.

The sampling of initial conditions in the chosen subspace is trivial. For other modes which are not included in the subspace, a reasonable choice is to assign the corresponding harmonic zero-point motion to each of them, perhaps with a random initial phase which helps to avoid possible bias and insufficient exploration of the configuration space. In some cases, one assigns no initial kinetic energy to some of the modes so as to avoid noisy spectrum.[30] In order to decrease the influence of nonincluded modes and the systematic errors introduced by the subspace division process, an appropriate criterion shall be applied. However, this will not be a problem in this paper since we are not making very fine divisions.

Cross-Correlation Filter Diagonalization Method. The cross-correlation matrix of reference states are defined similar to the surviving amplitude as

$$C_{ij}(t) \equiv \langle \chi_i|e^{-i\hat{H}t/\hbar}|\chi_j\rangle \quad (11)$$

It can be obtained on an equally spaced time grid by fixed-step semiclassical dynamics. Assuming $\hat{H}$ to be a Hamiltonian with discrete eigenvalues, the cross-correlations are supposed to be some linear combinations of harmonics

$$C_{ij}(t) = \sum_n d_{n,ij}e^{-i\omega_n t} \quad (12)$$

https://doi.org/10.1021/acs.jpca.3c00576
J. Phys. Chem. A 2023, 127, 2902−2911

We use FDMs to solve this harmonic inversion problem, i.e., to recover the parameters in (12) from the time-domain signals.[44] Thus, the whole method is called cross-correlation filter diagonalization (CCFD).

These matrix elements can be interpreted as inner products between reference states propagated by some time steps

$$C_{ij}((n-m)\tau) = \langle \hat{U}^m \chi_i, \hat{U}^n \chi_j \rangle \equiv S_{im,jn} \tag{13}$$

where $\hat{U}$ is the finite time propagator

$$\hat{U} \equiv e^{-i\hat{H}\tau/\hbar} \tag{14}$$

The corresponding state vectors span a Krylov subspace generated by $\hat{U}$

$$\mathcal{K}_N(\hat{U}, \{\chi_i\}) \equiv \text{span} \bigcup_i \{\chi_i, \hat{U}\chi_i, \hat{U}^2\chi_i, \cdots, \hat{U}^{N-1}\chi_i\} \tag{15}$$

The basis above is often very close to be linearly dependent when N is not small. But, by taking advantage of the implicit basis consisting of finite-time evolution of the reference states, one can get a better estimate to the exact eigenstates than merely combining explicit basis functions. The projection of an arbitrary state in this subspace can be expanded as

$$|\Psi\rangle = \sum_{i,m} B_{im} \hat{U}^m |\chi_i\rangle \tag{16}$$

On the other hand, the same quantities can also be regarded as the matrix elements of $\hat{U}^k$ with arbitrary integer k

$$U^k_{im,jn} \equiv \langle \hat{U}^m \chi_i | \hat{U}^k | \hat{U}^n \chi_j \rangle = C_{ij}((n+k-m)\tau) \tag{17}$$

Thus, by evaluating the cross-correlation functions, we readily obtain the elements of the overlap matrix $\mathbf{S}$ and the propagator matrix $\mathbf{U}$ under the specified basis. Then, by solving the generalized eigenvalue problem

$$U^k \mathbf{B} = \lambda \mathbf{S} \mathbf{B} \tag{18}$$

we obtain the eigenvalue $\lambda = \exp\{-ikE\tau/\hbar\}$ and the expansion coefficients $\{B_{im}\}$ of the corresponding eigenvector in the form of eq 16. Finally the frequencies are extracted as

$$\omega_n = \frac{i}{k\tau} \ln \lambda_n \tag{19}$$

and the amplitudes as

$$d_{n,ij} = \langle \chi_i | \Psi_n \rangle \langle \Psi_n | \chi_j \rangle \tag{20}$$

The above formalism works for cross-correlation functions generated by a Hermitian Hamiltonian and thus unitary propagators. For signals with complex frequencies, i.e., with a damping factor, one shall change the Hermitian inner product to a complex symmetric one. The overall derivation is very similar to the above one except for some minor changes.[44] For simple cases, the system will be adequately nondissipative so that the Hermitian version suffices. We note here that the method requires the Hamiltonian to be constant in time and have discrete eigenvalues, which make it infeasible when the conditions are violated by the nature of the system or the systematic error introduced in the cross-correlation calculations. But, for the systems studied later in this work, one can see from the ignorable imaginary part of the extracted frequencies that the Hermitian version works very well.

In solving the generalized eigenvalue problem in eq 18, the linear dependence of the basis needs to be taken care of in order to avoid numerical instability. One suitable method here is to filter eigenvectors by eigenvalues. The overlap matrix is diagonalized, and eigenvectors with eigenvalues smaller than a cutoff threshold will be discarded. Then the problem is considered and solved in the contracted subspace, with a smaller but linearly independent basis set.

In order to retain good resolution after the contraction, some modifications to the basis need to be carried out. One may choose the Fourier transformed basis[44]

$$|\Psi_i(\phi_\nu)\rangle \equiv \sum_{m=0}^{N-1} e^{im\tau\phi_\nu} \hat{U}^m |\chi_i\rangle \tag{21}$$

with ϕ_ν lying in a narrow band around the frequency of interest. This will significantly enhance the ratio of the eigenstates with energy in that range and is especially useful when the number of energy levels exceeds that of the reference states. In this way, the information obtained from other methods including frequencies and vibrational modes might help to better shape the calculation. However, in this paper we will use a slightly different approach. The references are chosen to form an orthonormal basis and is computed by diagonalizing the Hamiltonian estimated from a coarse Quantum Monte Carlo (QMC) sampling of the potential. The resulting energy spectra is not accurate, but it gives a good estimate (here we only require the overlap to be not too small) to the wave function of the eigenstates. Then we carry out the diagonalization method directly with the reference states and obtain all frequencies at once. The overlap of eigenstates with reference states helps to identify the vibrational mode corresponding to each frequency.

The estimated Hamiltonian is calculated under the basis composed of coherent states with chosen parameters. The width matrix Γ is chosen to coincide with the ground state under harmonic approximation to the potential energy surface, same as commonly used in the IVR method. The centers of the wave packets are chosen to be at the equilibrium positions. The momentum parameters are determined by

$$\mathbf{p} = c_1 \mathbf{p}_{\text{eq},i} + c_2 \mathbf{p}_{\text{eq},j} \tag{22}$$

Here $i \neq j$ is normal mode index, $\mathbf{p}_{\text{eq}}$ is the momentum along that normal mode with harmonic zero point energy, and $c_{1,2} \in \{-1/4, 0, +1/4\}$. The coefficient set is chosen as such that the combination of coherent states mimic the harmonic vibrational eigenstates, and thus we can expect a good estimation to the true eigenfunctions in the spanned space. It shall be noted again that we only need a mere approximation due to the use of implicit basis. It can also be expected that symmetries are preserved in the process, so one can easily assign symmetry indexes to the results.

RESULTS AND DISCUSSION

Water Monomer. The adiabatic potential energy surface we use for water in this paper is a newly developed one fitted by fundamental invariant neural network (FI-NN) which ensures invariant energy under atom permutations. For the monomer, the potentials come from the high-quality ab initio PES of Partridge and Schwenke.[50] The fitting error is 7.84×10^{-3} meV, which is negligible with respect to other sources of error. The many-body terms are constructed by using a many-body expansion method.[51] The two-body term is fitted from a large database of water dimer energies consisting of 220,000 data points computed at the CCSD(T) level and extrapolated

https://doi.org/10.1021/acs.jpca.3c00576
J. Phys. Chem. A 2023, 127, 2902−2911

to the CBS limit,[52,53] with a very small fitting error of 0.228 meV. For the three-body term, 430,000 data points at the CCSD(T)/AVTZ level are used. Trimer data points are fitted in two parts according to the median of O−O bond lengths and connected at 6−7 Å. The fitting errors are 0.347 meV for short range and 0.027 meV for long range. To remove the basis set superposition error (BSSE), the counterpoise method is applied.[54]

There is one global minimum which corresponds to the well-known geometric structure of a water molecule. The harmonic frequencies are computed at this equilibrium position, which then decides the width matrix in further IVR calculations. The Divide-and-Conquer technique is unnecessary and will not be used for this 3-dimensional system. For comparison, TA-SC-IVR calculations are carried out for each normal mode with trajectories up to 10^4 a.u. long, and results are shown in Table 1. Vibrational modes are labeled in ascending order in terms of magnitude, from lower to higher being bending, symmetric stretching, and asymmetric stretching modes. The TA results are much better than harmonic approximations, which is expected because of the capability of IVR to partly describe anharmonic effects. When it comes to CCFD calculation, the trajectories are evolved for a maximum length of 120 steps with 10 a.u. each step. Initial positions and momenta are sampled by the Metropolis algorithm, with the probability distribution chosen to be the module of the overlap coefficient of the coherent state to the zeroth reference state. A whole collection of cross-correlation functions are calculated from this trajectory set. Part of them are plotted in Figure 1. The QMC estimate is passable in this case, so the matrix elements between different reference states are relatively small. From the diagonal, one can see their surviving amplitudes "leak" since they are not the exact eigenstates. But it is well enough for FDM to extract eigenvalues. The extracted frequencies are also listed in Table 1. The CCFD results are very close to, and even have a better MAE than, the time-averaging IVR results. This indicates that the short-time correlation functions carry the correct frequency information.

To investigate the effect of total evolution time, the relation between the maximum trajectory length and the final results are plotted in Figure 2. As can be seen, a total time of 1200 a.u. is sufficient for convergence in this case. At this time scale, the statistical error has been suppressed to less than 2 cm^{-1}, which can be ignored with respect to the mean total error. Thus, the method is accurate enough while working with short trajectories. To further inspect convergence of the method, frequencies extracted from an increasing number of evolved

Table 1. Water Monomer Vibrational Spectrum Calculated with Different Methods[a]

Mode	Expt.	Harm.	TA-SC-IVR	CCFD
1_1	1595	1649	1586	1586
1_2	3152	3298	3136	3134
2_1	3657	3837	3665	3653
3_1	3756	3955	3766	3755
MAE		144	11	8

[a]Energies are in wavenumbers (cm^{-1}).

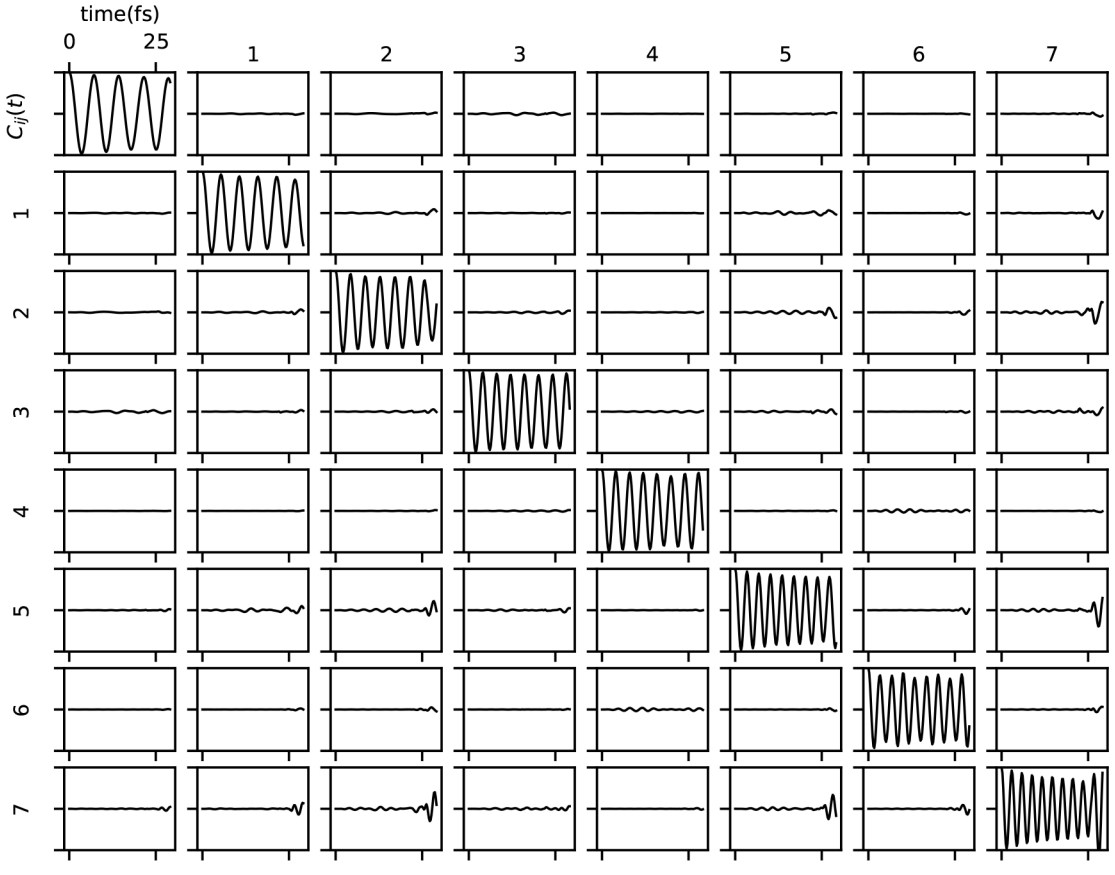

Figure 1. Real part of cross-correlation functions of the first 8 reference states. The labels on rows and columns denote *i*, *j*.

https://doi.org/10.1021/acs.jpca.3c00576
J. Phys. Chem. A 2023, 127, 2902−2911

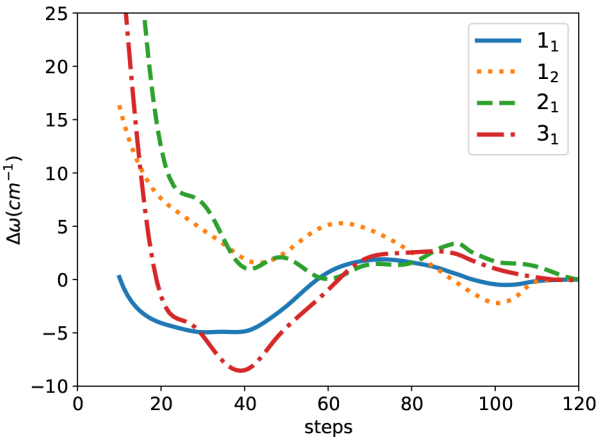

Figure 2. Convergence plot of the four frequencies with increasing evolving time. The result at 120 steps (1200 a.u.) is taken as reference.

trajectories are plotted in Figure 3. It is shown that a total number of 20,000 trajectories is enough for a stable result and

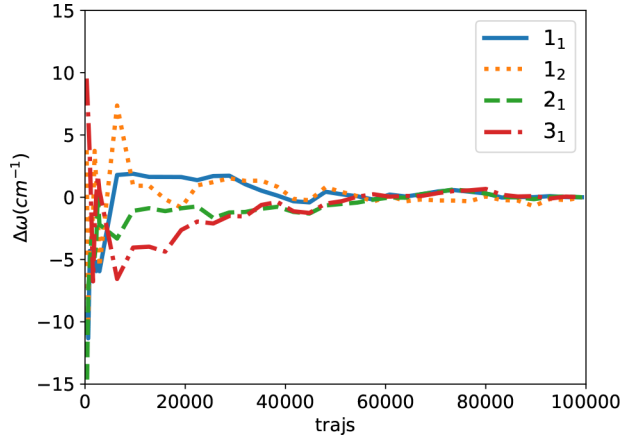

Figure 3. Convergence plot of the four frequencies with increasing number of trajectories evolved. The result at 10^5 is taken as reference.

40,000 is sufficient for convergence. This is slightly larger than that with typical IVR calculations but still at the same order.[29] Thus, the total computational cost is lowered due to the significant reduce of the trajectory length. The distribution of singular values of the overlap matrix **S** is shown in Figure 4. The upper half contains 16 values for each instance of **S**, the same number as the reference states we used in the cross-correlation calculation, while the total number of singular values grows linearly with time steps. The obvious separation of the two halves indicates that the subspace spanned by the states estimated from the QMC preprocessing is close to the exact one. Since most values pile up at the bottom, we only need to take the few larger ones in the lower half and cut others off from further calculation. In fact, the results are fairly insensitive to the cutoff value as long as the upper half is kept.

Methane Molecule. The results in this section are all based on the same accurate ab initio force field of Lee–Martin–Taylor (LMT) in internal symmetry coordinates, as presented in ref 55. The global minimum is the regular tetrahedron configuration, which has T_d symmetry. For this PES, full-dimensional quantum results are available which use MULTIMODE to calculate rovibrational energies variationally.[56] The method has been tested on four-atom systems and

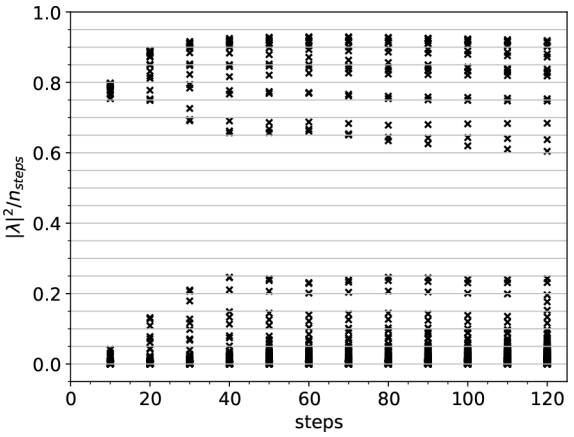

Figure 4. Distribution of singular values of the overlapping matrix divided by number of steps.

has shown results in quantitative agreement with full variational calculations or grid method. Thus, we are taking it as a quantum benchmark here. The configuration of classical dynamics in CCFD is the same as for water monomer, except for a total dimension of 9 vibrational modes. The system is reported to be very chaotic and most of the trajectories have to be discarded in long-time evolution.[29] However, in CCFD, the ratio of rejected trajectories is negligible because the total evolution time is significantly shortened.

When it comes to degeneracy, the CCFD results show the correct number of degenerate frequencies even though we did not do any explicit symmetrization operations. Symmetry and degeneracy just naturally arise during the simulation. For fundamentals, each mode corresponds to an irreducible representation, while for overtones the symmetrized products factorize into smaller representations and the energy level is split. In both cases, the CCFD results consist of groups of very close values, which are still slightly different due to statistical fluctuation. Their sizes are exactly the dimension of the irreducible representations. Thus, we can easily assign symmetry labels without ambiguity.

For comparison with the MULTIMODE benchmark, we are taking the average of the obtained energies which correspond to the same mode index as the result. Previous studies that used the Divide-and-Conquer IVR method or the Adiabatic Switching method are also taken into comparison.[29,35] These results are shown in the left half of Table 2. The CCFD results have a very high accuracy with respect to the benchmark values. Again, correct frequencies are extracted from short-time dynamics, and the result is even better than other IVR methods. For further study of finer recognition of split overtones, another benchmark is used which features the Lanczos algorithm.[57] Results are shown in the right half of Table 2. The CCFD results are in very good agreement with the quantum variational method, proving its ability to identify very closely spaced peaks. The same mean error is found in the detailed comparison, providing evidence that the accuracy of CCFD results is no coincidence.

Water Trimer. The force field we use here is the same as for water monomer, with multibody terms used. These terms are absent in the case of monomer. The normal modes are calculated at the global minimum configuration, i.e., the up–up–down (uud) structure of the trimer.[58] The Divide-and-Conquer technique is applied, and only the 9 intramolecular vibrational modes which have the highest frequencies are

https://doi.org/10.1021/acs.jpca.3c00576
J. Phys. Chem. A 2023, 127, 2902–2911

Table 2. Methane Molecule Vibrational Spectrum Calculated with Different Methods, with the Energies Presented in Wave Numbers (cm^{-1})

Mode	MM[a]	Harm.	DC-SC-IVR[b]	AS-SC-IVR[c]	CCFD	Rep.	Lanczos[d]	CCFD
4_1	3053	3165	3044	3058	3058	F_2	3055	3058
2_2	3067	3148	3050		3073	E	3069	3073
						A_1	3062	3058
3_1	2949	3043	2964	2950	2948	A_1	2955	2948
1_12_1	2836	2923	2834	2839	2843	F_1	2852	2848
						F_2	2839	2838
1_2	2624	2690	2606	2614	2619	E	2639	2636
						F_2	2628	2616
						A_1	2599	2595
2_1	1535	1574	1532	1530	1537	E	1535	1537
1_1	1313	1349	1300	1307	1315	F_2	1315	1315
MAE-MM		74	11	5	4	MAE-Lanczos		4

[a]MULTIMODE result.[56] [b]Previous result by Di Liberto et al.[29] from the same force field and with the Divide-and-Conquer technique, which has the best MAE among listed methods there. [c]Previous result by Conte et al.[35] from the same force field and with Adiabatic Switching technique. [d]Lanczos result.[57]

included in the subspace. There are 6 modes of OH bond stretching and 3 modes of bending, and they are the only modes of interest here. Other modes are given zero initial energy. In long-time calculations, the subspace is further limited to one-dimensional, with the other 8 modes assigned with zero-point motion. The result is compared to experiment,[59] MULTIMODE,[60] and long-time DC-SC-IVR in Table 3. Our DC-SC-IVR and DC-CCFD calculations both use the PES mentioned above, and MULTIMODE results are based on the WHBB potential. This time we are directly using the experimental values as benchmark not only because of the difference on potentials but also due to the fact that MULTIMODE calculation is not full-dimensional for the large system with 21 modes and is no longer guaranteed to have very good accuracy.

Table 3. Water Trimer Vibrational Spectrum Calculated with Different Methods, with the Energies Presented in Wave Numbers (cm^{-1})

Expt.	Harm.	MM[a]	DC-SC-IVR	DC-CCFD
	Mode 19−21: Free OH Stretch			
3722	3922	3720	3795	3746
	3922	3715	3718	3737
	3917	3709	3641	3731
	Mode 16−18: H-Bonded OH Stretch			
3452	3698	3514	3487	3466
3434	3690	3504	3465	3456
3410/3398	3636	3486	3509	3393
	Mode 13−15: Bendings			
1608	1688	1623	1639	1643
	1666	1600	1617	1620
	1664	1597	1606	1610
MAE	169	30	41	16

[a]MULTIMODE result.[60]

None of the methods successfully predicted the quartet bands of single-donor hydrogen-bonded OH stretch near 3400 cm^{-1}. They all end up with only 3 eigenvalues in this region. The reason for this phenomena might be the neglect of the libration modes, which can cause tunneling splittings in the rovibrational spectrum, or insufficient consideration of single-molecule rotation in the potential energy surface. But, from the peak spacing, one can reasonably assign the two lowest frequencies to the same mode in Table 3.

The DC-CCFD results are quite accurate for all the nine levels. The major advantage is found on the results for modes 16−18. The same trend is seen in both MULTIMODE and DC-SC-IVR results that there is rather large error for these single-donor hydrogen-bonded modes. But, with DC-CCFD, the results are as good as other modes. The calculated frequencies and the experimental spectrum are demonstrated in Figure 5, from which one can clearly see the difference. Due to the fact that we do not have the same WHBB potential to perform the DC-CCFD simulations, the difference between MULTIMODE and DC-CCFD cannot be analyzed in a very clear manner. Therefore, we attribute this agreement with experimental data to the combined use of the high precision of the potential energy surface and the DC-CCFD method. For readers interested in the scalability of the method with the number of degrees of freedom, we note in passing here that the total computational time is around 120 CPU hours for the calculation of water monomer and about 2600 CPU hours for the trimer. This is within expectation because we need to calculate the Hessian matrix.

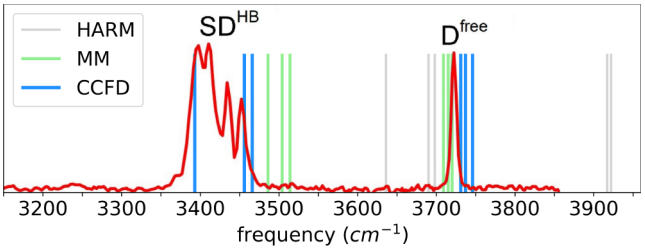

Figure 5. Demonstrative plot of IR spectra of water trimer from experiment[59] and the calculated frequencies. D^{free} denotes donor-free OH stretch (mode 19−21) while SD^{HB} denotes single-donor hydrogen-bonded OH stretch (mode 16−18). The two harmonic lines on the right belongs to D^{free} (with degeneracy) and the rest belongs to SD^{HB}. The MULTIMODE (MM) and DC-CCFD (CCFD) results are just accurate enough to identify.

https://doi.org/10.1021/acs.jpca.3c00576
J. Phys. Chem. A 2023, 127, 2902−2911

CONCLUSION

In this paper, we implemented the SC-IVR with FDM and investigated the vibrational spectrum of water monomer, methane molecule, and water clusters. The total evolving time of classical trajectories is tremendously shortened with respect to conventional IVR methods based on Fourier transformation. The reduction in the number of steps decreases the computational cost and results in better numerical stability and accuracy. For water monomer and methane molecule, a full-dimensional calculation is performed to get all vibrational frequencies in one run. For the case of water trimer, the Divide-and-Conquer technique is used to restrict the total dimension to 9. The final results are very encouraging, proving the reliability of this short-time method. It makes us confident that this method can work effectively on real molecular systems and high-precision potential energy surfaces. To further improve the accuracy and applicability of the method, future studies may explore the feasibility of combining it with ab initio molecular dynamics, possibly with new techniques and improvements. In the future, it might be a powerful tool for vibrational spectral investigation.

AUTHOR INFORMATION

Corresponding Authors

Yu-Cheng Zhu − *State Key Laboratory for Artificial Microstructure and Mesoscopic Physics, Frontier Science Center for Nano-optoelectronics, School of Physics, Peking University, Beijing 100871, People's Republic of China;* orcid.org/0000-0003-2255-025X; Email: zhuyucheng@pku.edu.cn

Xin-Zheng Li − *State Key Laboratory for Artificial Microstructure and Mesoscopic Physics, Frontier Science Center for Nano-optoelectronics, School of Physics, Peking University, Beijing 100871, People's Republic of China; Interdisciplinary Institute of Light-Element Quantum Materials, Research Center for Light-Element Advanced Materials, and Collaborative Innovation Center of Quantum Matter, Peking University, Beijing 100871, People's Republic of China; Peking University Yangtze Delta Institute of Optoelectronics, Nantong, Jiangsu 226010, People's Republic of China;* orcid.org/0000-0003-0316-4257; Email: xzli@pku.edu.cn

Authors

Jia-Xi Zeng − *State Key Laboratory for Artificial Microstructure and Mesoscopic Physics, Frontier Science Center for Nano-optoelectronics, School of Physics, Peking University, Beijing 100871, People's Republic of China*

Shuo Yang − *State Key Laboratory of Molecular Reaction Dynamics, Dalian Institute of Chemical Physics, Chinese Academy of Sciences, Dalian 116023, People's Republic of China; University of Chinese Academy of Sciences, Beijing 100049, People's Republic of China*

Wei Fang − *State Key Laboratory of Molecular Reaction Dynamics, Dalian Institute of Chemical Physics, Chinese Academy of Sciences, Dalian 116023, People's Republic of China; Department of Chemistry, Fudan University, Shanghai 200438, People's Republic of China*

Ling Jiang − *State Key Laboratory of Molecular Reaction Dynamics, Dalian Institute of Chemical Physics, Chinese Academy of Sciences, Dalian 116023, People's Republic of China;* orcid.org/0000-0002-8485-8893

En-Ge Wang − *International Center for Quantum Materials and School of Physics, Peking University, Beijing 100871, People's Republic of China; Songshan Lake Materials Lab, Institute of Physics, Chinese Academy of Science, Dongguan, Guangdong 523808, People's Republic of China*

Dong H. Zhang − *State Key Laboratory of Molecular Reaction Dynamics, Dalian Institute of Chemical Physics, Chinese Academy of Sciences, Dalian 116023, People's Republic of China;* orcid.org/0000-0001-9426-8822

Complete contact information is available at: https://pubs.acs.org/10.1021/acs.jpca.3c00576

Notes

The authors declare no competing financial interest.

ACKNOWLEDGMENTS

We are supported by the National Science Foundation of China under Grant No. 11934003, 11888101, 12234001, the Guangdong Major Project of Basic and Applied Basic Research (2021B0301030002), the National Basic Research Programs of China under Grant No. 2021YFA1400503, the Beijing Natural Science Foundation under Grant No. Z200004, and the Strategic Priority Research Program of the Chinese Academy of Sciences Grant No. XDB33010400. The computational resources were provided by the supercomputer center in Peking University, China.

REFERENCES

(1) Berens, P. H.; Wilson, K. R. Molecular dynamics and spectra. I. Diatomic rotation and vibration. *J. Chem. Phys.* **1981**, *74*, 4872−4882.

(2) Guillot, B. A molecular dynamics study of the far infrared spectrum of liquid water. *J. Chem. Phys.* **1991**, *95*, 1543−1551.

(3) Bosma, W. B.; Fried, L. E.; Mukamel, S. Simulation of the intermolecular vibrational spectra of liquid water and water clusters. *J. Chem. Phys.* **1993**, *98*, 4413−4421.

(4) Gaigeot, M.-P.; Sprik, M. Ab Initio Molecular Dynamics Computation of the Infrared Spectrum of Aqueous Uracil. *J. Phys. Chem. B* **2003**, *107*, 10344−10358.

(5) Thomas, M.; Brehm, M.; Fligg, R.; Vöhringer, P.; Kirchner, B. Computing vibrational spectra from ab initio molecular dynamics. *Phys. Chem. Chem. Phys.* **2013**, *15*, 6608−6622.

(6) Alimi, R.; García-Vela, A.; Gerber, R. B. A remedy for zero-point energy problems in classical trajectories: A combined semiclassical/classical molecular dynamics algorithm. *J. Chem. Phys.* **1992**, *96*, 2034−2038.

(7) Wu, F.; Ren, Y.; Bian, W. The hydrogen tunneling splitting in malonaldehyde: A full-dimensional time-independent quantum mechanical method. *J. Chem. Phys.* **2016**, *145*, 074309.

(8) Tremblay, B.; Madebène, B.; Alikhani, M.; Perchard, J. The vibrational spectrum of the water trimer: Comparison between anharmonic ab initio calculations and neon matrix infrared date between 11,000 and 90 cm-1. *Chem. Phys.* **2010**, *378*, 27−36.

(9) Richardson, J. O.; Pérez, C.; Lobsiger, S.; Reid, A. A.; Temelso, B.; Shields, G. C.; Kisiel, Z.; Wales, D. J.; Pate, B. H.; Althorpe, S. C. Concerted hydrogen-bond breaking by quantum tunneling in the water hexamer prism. *Science* **2016**, *351*, 1310−1313.

(10) Meyer, H.-D.; Manthe, U.; Cederbaum, L. The multi-configurational time-dependent Hartree approach. *Chem. Phys. Lett.* **1990**, *165*, 73−78.

(11) Manthe, U.; Meyer, H.-D.; Cederbaum, L. S. Wave-packet dynamics within the multiconfiguration Hartree framework: General aspects and application to NOCl. *J. Chem. Phys.* **1992**, *97*, 3199−3213.

(12) Beck, M.; Meyer, H.-D. An efficient and robust integration scheme for the equations of motion of the multiconfiguration time-

dependent Hartree (MCTDH) method. *Z. Phys. D: At. Mol. Clusters* **1997**, *42*, 113−129.
(13) Beck, M.; Jäckle, A.; Worth, G.; Meyer, H.-D. The multiconfiguration time-dependent Hartree (MCTDH) method: a highly efficient algorithm for propagating wavepackets. *Phys. Rep.* **2000**, *324*, 1−105.
(14) Bowman, J. M. Self-consistent field energies and wavefunctions for coupled oscillators. *J. Chem. Phys.* **1978**, *68*, 608−610.
(15) Bowman, J. M.; Christoffel, K.; Tobin, F. Application of SCF-SI theory to vibrational motion in polyatomic molecules. *J. Phys. Chem.* **1979**, *83*, 905−912.
(16) Christoffel, K. M.; Bowman, J. M. Investigations of self-consistent field, scf ci and virtual state configuration interaction vibrational energies for a model three-mode system. *Chem. Phys. Lett.* **1982**, *85*, 220−224.
(17) Carter, S.; Culik, S. J.; Bowman, J. M. Vibrational self-consistent field method for many-mode systems: A new approach and application to the vibrations of CO adsorbed on Cu(100). *J. Chem. Phys.* **1997**, *107*, 10458−10469.
(18) Bowman, J. M.; Carrington, T.; Meyer, H.-D. Variational quantum approaches for computing vibrational energies of polyatomic molecules. *Mol. Phys.* **2008**, *106*, 2145−2182.
(19) Grimm, R.; Storer, R. Monte-Carlo solution of Schr?dinger's equation. *J. Comput. Phys.* **1971**, *7*, 134−156.
(20) Badinski, A.; Haynes, P. D.; Needs, R. J. Nodal Pulay terms for accurate diffusion quantum Monte Carlo forces. *Phys. Rev. B* **2008**, *77*, 085111.
(21) Needs, R. J.; Towler, M. D.; Drummond, N. D.; Ríos, P. L. Continuum variational and diffusion quantum Monte Carlo calculations. *J. Phys.: Condens. Matter* **2010**, *22*, 023201.
(22) Craig, I. R.; Manolopoulos, D. E. Quantum statistics and classical mechanics: Real time correlation functions from ring polymer molecular dynamics. *J. Chem. Phys.* **2004**, *121*, 3368−3373.
(23) Hone, T. D.; Rossky, P. J.; Voth, G. A. A comparative study of imaginary time path integral based methods for quantum dynamics. *J. Chem. Phys.* **2006**, *124*, 154103.
(24) Witt, A.; Ivanov, S. D.; Shiga, M.; Forbert, H.; Marx, D. On the applicability of centroid and ring polymer path integral molecular dynamics for vibrational spectroscopy. *J. Chem. Phys.* **2009**, *130*, 194510.
(25) Miller, W. H.; Classical, S. Matrix: Numerical Application to Inelastic Collisions. *J. Chem. Phys.* **1970**, *53*, 3578−3587.
(26) Herman, M. F.; Kluk, E. A semiclasical justification for the use of non-spreading wavepackets in dynamics calculations. *Chem. Phys.* **1984**, *91*, 27−34.
(27) van Vleck, J. H. The Correspondence Principle in the Statistical Interpretation of Quantum Mechanics. *Proc. Natl. Acad. Sci. U.S.A.* **1928**, *14*, 178−188.
(28) Ceotto, M.; Di Liberto, G.; Conte, R. Semiclassical "Divide-and-Conquer" Method for Spectroscopic Calculations of High Dimensional Molecular Systems. *Phys. Rev. Lett.* **2017**, *119*, 010401.
(29) Di Liberto, G.; Conte, R.; Ceotto, M. Divide and conquer" semiclassical molecular dynamics: A practical method for spectroscopic calculations of high dimensional molecular systems. *J. Chem. Phys.* **2018**, *148*, 014307.
(30) Di Liberto, G.; Conte, R.; Ceotto, M. Divide-and-conquer" semiclassical molecular dynamics: An application to water clusters. *J. Chem. Phys.* **2018**, *148*, 104302.
(31) Gabas, F.; Conte, R.; Ceotto, M. Semiclassical Vibrational Spectroscopy of Biological Molecules Using Force Fields. *J. Chem. Theory Comput.* **2020**, *16*, 3476−3485.
(32) Kaledin, A. L.; Miller, W. H. Time averaging the semiclassical initial value representation for the calculation of vibrational energy levels. *J. Chem. Phys.* **2003**, *118*, 7174−7182.
(33) Kaledin, A. L.; Miller, W. H. Time averaging the semiclassical initial value representation for the calculation of vibrational energy levels. II. Application to H2CO,NH3, CH4,CH2D2. *J. Chem. Phys.* **2003**, *119*, 3078−3084.
(34) Ceotto, M.; Tantardini, G. F.; Aspuru-Guzik, A. Fighting the curse of dimensionality in first-principles semiclassical calculations: Non-local reference states for large number of dimensions. *J. Chem. Phys.* **2011**, *135*, 214108.
(35) Conte, R.; Parma, L.; Aieta, C.; Rognoni, A.; Ceotto, M. Improved semiclassical dynamics through adiabatic switching trajectory sampling. *J. Chem. Phys.* **2019**, *151*, 214107.
(36) Botti, G.; Ceotto, M.; Conte, R. On-the-fly adiabatically switched semiclassical initial value representation molecular dynamics for vibrational spectroscopy of biomolecules. *J. Chem. Phys.* **2021**, *155*, 234102.
(37) Conte, R.; Gabas, F.; Botti, G.; Zhuang, Y.; Ceotto, M. Semiclassical vibrational spectroscopy with Hessian databases. *J. Chem. Phys.* **2019**, *150*, 244118.
(38) Garashchuk, S.; Light, J. C. Simplified calculation of the stability matrix for semiclassical propagation. *J. Chem. Phys.* **2000**, *113*, 9390−9392.
(39) Di Liberto, G.; Ceotto, M. The importance of the pre-exponential factor in semiclassical molecular dynamics. *J. Chem. Phys.* **2016**, *145*, 144107.
(40) Markovich, T.; Blau, S. M.; Sanders, J. N.; Aspuru-Guzik, A. Benchmarking compressed sensing, super-resolution, and filter diagonalization. *Int. J. Quantum Chem.* **2016**, *116*, 1097−1106.
(41) Wall, M. R.; Neuhauser, D. Extraction, through filter-diagonalization, of general quantum eigenvalues or classical normal mode frequencies from a small number of residues or a short-time segment if a signal. I. Theory and application to a quantum-dynamics model. *J. Chem. Phys.* **1995**, *102*, 8011−8022.
(42) Pang, J. W.; Dieckmann, T.; Feigon, J.; Neuhauser, D. Extraction of spectral information from a short-time signal using filter-diagonalization: Recent developments and applications to semi-classical reaction dynamics and nuclear magnetic resonance signals. *J. Chem. Phys.* **1998**, *108*, 8360−8368.
(43) Mandelshtam, V. A.; Taylor, H. S. Harmonic inversion of time signals and its applications. *J. Chem. Phys.* **1997**, *107*, 6756−6769.
(44) Mandelshtam, V. FDM: the filter diagonalization method for data processing in NMR experiments. *Prog. Nucl. Magn. Reson. Spectrosc.* **2001**, *38*, 159−196.
(45) Narevicius, E.; Neuhauser, D.; Jürgen Korsch, H.; Moiseyev, N. Resonances from short time complex-scaled cross-correlation probability amplitudes by the filter-diagonalization method. *Chem. Phys. Lett.* **1997**, *276*, 250−254.
(46) Anderson, S. M.; Ka, J.; Felker, P. M.; Neuhuaser, D. Semi-classical versus exact eigenvalues of He-benzene using cross-correlation filter-diagonalization. *Chem. Phys. Lett.* **2000**, *328*, 516−521.
(47) Giese, K.; Kühn, O. Semiclassical tunneling splittings from short time dynamics: Herman-Kluk-propagation and harmonic inversion. *J. Chem. Phys.* **2004**, *120*, 4107−4118.
(48) Miller, W. H. The Semiclassical Initial Value Representation: A Potentially Practical Way for Adding Quantum Effects to Calssical Molecular Dynamics Simulations. *J. Phys. Chem. A* **2001**, *105*, 2942−2955.
(49) Miller, W. H. *Adv. Chem. Phys.*; John Wiley & Sons, Ltd., 1974; pp 69−177.
(50) Partridge, H.; Schwenke, D. W. The determination of an accurate isotope dependent potential energy surface for water from extensive ab initio calculations and experimental data. *J. Chem. Phys.* **1997**, *106*, 4618−4639.
(51) Hankins, D.; Moskowitz, J. W.; Stillinger, F. H. Water Molecule Interactions. *J. Chem. Phys.* **1970**, *53*, 4544−4554.
(52) Halkier, A.; Klopper, W.; Helgaker, T.; Jørgensen, P.; Taylor, P. R. Basis set convergence of the interaction energy of hydrogen-bonded complexes. *J. Chem. Phys.* **1999**, *111*, 9157−9167.
(53) Halkier, A.; Helgaker, T.; Jørgensen, P.; Klopper, W.; Olsen, J. Basis-set convergence of the energy in molecular Hartree-Fock calculations. *Chem. Phys. Lett.* **1999**, *302*, 437−446.

https://doi.org/10.1021/acs.jpca.3c00576
J. Phys. Chem. A 2023, 127, 2902−2911

(54) Boys, S.; Bernardi, F. The calculation of small molecular interactions by the differences of separate total energies. Some procedures with reduced errors. *Mol. Phys.* **1970**, *19*, 553−566.
(55) Lee, T. J.; Martin, J. M. L.; Taylor, P. R. An accurate ab initio quartic force field and vibrational frequencies for CH4 and isotopomers. *J. Chem. Phys.* **1995**, *102*, 254−261.
(56) Carter, S.; Shnider, H. M.; Bowman, J. M. Variational calculations of rovibrational energies of CH4 and isotopomers in full dimensionality using an ab initio potential. *J. Chem. Phys.* **1999**, *110*, 8417−8423.
(57) Yu, H.-G. An exact variational method to calculate vibrational energies of five atom molecules beyond the normal mode approach. *J. Chem. Phys.* **2002**, *117*, 2030−2037.
(58) Keutsch, F. N.; Cruzan, J. D.; Saykally, R. J. The Water Trimer. *Chem. Rev.* **2003**, *103*, 2533−2578.
(59) Zhang, B.; et al. Infrared spectroscopy of neutral water clusters at finite temperature: Evidence for a noncyclic pentamer. *Proc. Natl. Acad. Sci. U.S.A.* **2020**, *117*, 15423−15428.
(60) Wang, Y.; Bowman, J. M. Ab initio potential and dipole moment surfaces for water. II. Local-monomer calculations of the infrared spectra of water clusters. *J. Chem. Phys.* **2011**, *134*, 154510.

https://doi.org/10.1021/acs.jpca.3c00576
J. Phys. Chem. A 2023, 127, 2902−2911